Available online at www.sciencedirect.com
SCIENCE DIRECT
Journal of Sound and Vibration 293 (2006) 953–964
JOURNAL OF SOUND AND VIBRATION
www.elsevier.com/locate/jsvi

Derivation of train track isolation requirement for a steel road bridge based on vibro-acoustic analyses

F. Augusztinovicz*, F. Márki, K. Gulyás, A.B. Nagy, P. Fiala, P. Gajdátsy

Department of Telecommunications, Budapest University of Technology and Economics, H-1117 Budapest, Magyar tudósok körútja 2, Hungary

Accepted 26 August 2005
Available online 30 January 2006

Abstract

The paper reports on a hybrid method, aimed at predicting the expected noise emission of the structure-borne component of a combined bridge/track system, currently under development. The method is based on detailed vibro-acoustic analyses of the bridge and consists of three major elements: experimental estimation of input dynamic forces generated by rolling of trams along the track; a detailed analysis of the steel box girder bridge structure based both on experiments and numerical calculations; and estimation of sound radiation from the bridge structure performed by means of boundary element methods and validated on the bridge by vibro-acoustic measurements. The proposed method was used for the hypothetical case that no vibration isolation is installed and it was established that at least 10–12 dB(A) noise reduction is required. As reported elsewhere, the calculation can be repeated for isolated tracks and the efficiency of various track design versions can be evaluated.

1. Introduction

The Lágymányosi bridge of Budapest was constructed between 1992 and 1995. It forms part of a major boulevard across the Danube in the Southern part of the Hungarian capital and carries heavy traffic as from its inauguration (on average approx. 5400 cars and 350 lorries and trucks per hour). A tram track in the middle of the bridge was also planned and made ready for installation, but not completed so far. In the meantime, traffic demand has made the construction of the tram track along the bridge inevitable but, due to the ongoing construction of very demanding cultural buildings in the close vicinity of the bridge, the design of the vibration insulation of the track had to be revised. This paper reports on the investigations aimed at deriving isolation requirements, the fulfilment of which is required to avoid significant noise level increase in the area.

The bridge investigated is a 495 m long, continuous beam box girder steel bridge, with orthotropic deck plate, see Fig. 1. [1]. As discussed elsewhere [2], the total noise, including both airborne and structure-borne component of the new tram line running along the bridge, may not generate higher equivalent noise levels than

*Corresponding author. Fax: +36 1 463 3266.
E-mail address: fulop@hit.bme.hu (F. Augusztinovicz).

0022-460X/$ - see front matter © 2006 Elsevier Ltd. All rights reserved.
doi:10.1016/j.jsv.2005.12.018

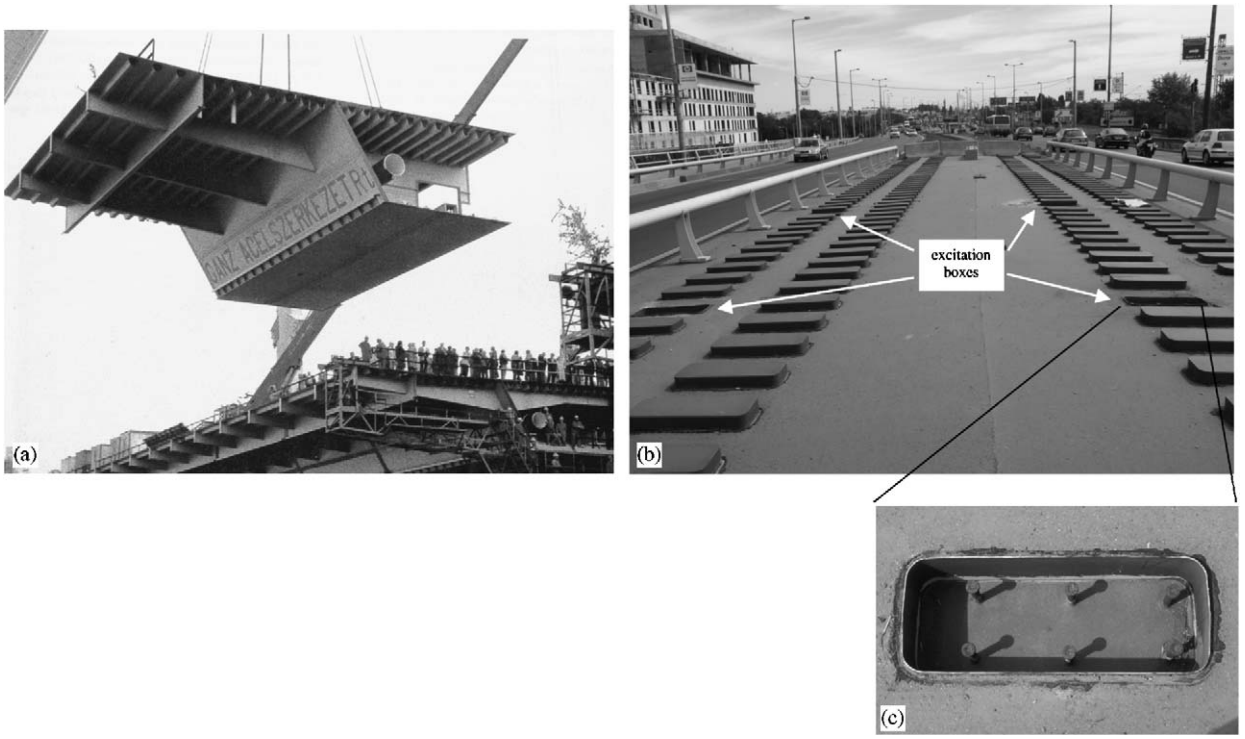

Fig. 1. The Lágymányosi bridge in Budapest. (a) Lifting in of the last bridge element in May 1993 [1]; (b) Part of the prepared tram track in the middle of the bridge, selected for experiments. Each box consists of six steel mandrels, welded directly to the deck plate. Four boxes (denoted by arrows) have been opened for measurements. (c) Steel mandrels within one of the open boxes, used for impact excitation of the bridge structure.

62 dB(A) for the day and 59 dB(A) for the night along the most critical façade of the Palace of the Arts situated at just 30 m distance from the abutement. In addition to this, it was generally accepted both by the investor and designers of Palace of the Arts that the acoustical planning of the critical rooms should be based on short-time maximum values rather than just full-day of full-night equivalent noise limits, making the requirements even more stringent.

Due to the relatively soft but bulky steel structure of the bridge in question, there is no doubt that the structure-borne noise component of the bridge would be predominant with respect to the pure airborne noise of the trams, with probably even larger difference than for typical railway bridges (usually 8–12 dB excess for truss railway bridges, see e.g. in Ref. [3]). Investigations have therefore concentrated on the structure-borne component of the tram noise, aimed at revealing the radiation mechanisms of the bridge structure, developing a prediction method to estimate the structure-borne noise and to define the necessary vibration isolation to keep the structure-borne component at an acceptable level.

2. Vibro-acoustic analysis of the bridge

The noise of steel railway bridges has attracted quite some interest in the last decade. The large majority of existing methods, see e.g. in Refs. [4–6], are analytical approaches for simple cases, or have been developed and verified for typical truss railway bridges. In the present case, however, all load-carrying structures of the bridge act as large noise radiating surfaces as well. Essential parts of the bridge are constructed of orthotropic plates, one of them (i.e. the deck plate) is covered with a thick layer of asphalt; all these need special attention in the course of modelling the bridge and calculating noise radiation.

Therefore, rather than using just one or another analytical or numerical approach, a number of different approaches were evaluated and eventually a hybrid method, consisting of both experimental and numerical techniques, was developed and applied for the problem, as discussed in Section 4.

2.1. Experiments on the bridge

Two series of measurements were performed on a 12 m long section of the bridge structure, bounded by two adjacent bulkheads. The bridge was excited through a number of steel mandrels, welded directly to the deck plate as part of the originally prepared track system and protected against environmental influences by steel boxes, see Fig. 1b and c. The measurements have taken place in the night-time hours of two consecutive days, with total closure of the bridge and all connecting roads for traffic. (Note that even at night the measurement time was very much limited, and no measurements could be extended or repeated afterwards.) The cross-section of the bridge together with positioning of the sensors is depicted in Fig. 2.

In the first series of measurements, the excitation was performed by an instrumented impact hammer from within two boxes just above a bulkhead on the left and right side of the bridge, and another two between the two bulkheads. The vibration of the bridge plates were measured at 33 points distributed along the section. All mandrels in each box were hit consecutively, and the transfer functions obtained were averaged. As a result, a matrix of 4×33 acceleration per force FRFs was generated.

A quick analysis of the recorded data has revealed that the bridge response most likely extends beyond the specified operating frequency range of the impact hammer used. Therefore, in the second set of measurements the excitation took place at the same points but using both instrumented and a simple steel hammer. One reference vibration on the deck plate and sound pressures at six points along a close proximity vertical line were measured.

2.1.1. Vibration measurements

Fig. 3a shows the structural response of the bridge, expressed in terms of the average vibration velocity per input force transfer function. As can be seen, the structure has a number of sharp resonances, the most important ones falling in the range between 30–80 Hz and above 600 Hz. It should be noted however that, according to the coherence functions, for example shown in Fig. 3b, the reliability of vibration FRFs is somewhat in doubt above about 600 Hz, and the results certainly cannot be used above 800 Hz. The reasons for this are twofold. Firstly, the PCB-type impact hammers used are limited in frequency range to 1000 Hz. Secondly, the steel structure investigated is very reverberant and hence, given the relatively short recording time determined by the very much limited measurement possibilities, it was difficult to obtain FRF data of good quality.

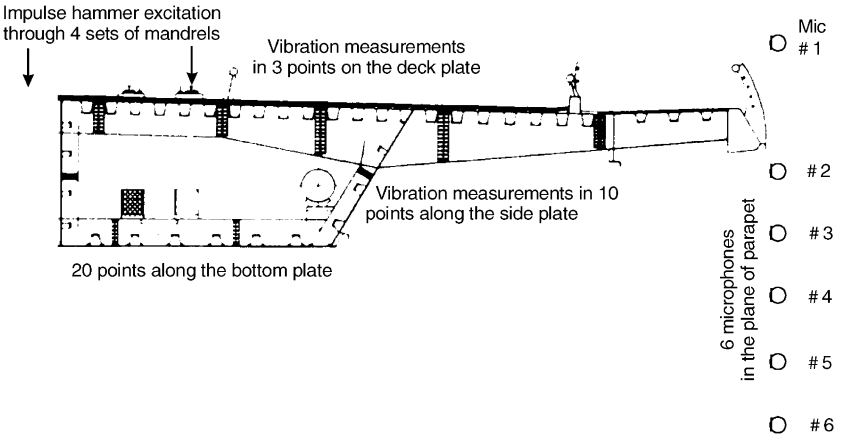

Fig. 2. Cross-section of the northern half of the bridge and position of sensors for the measurements.

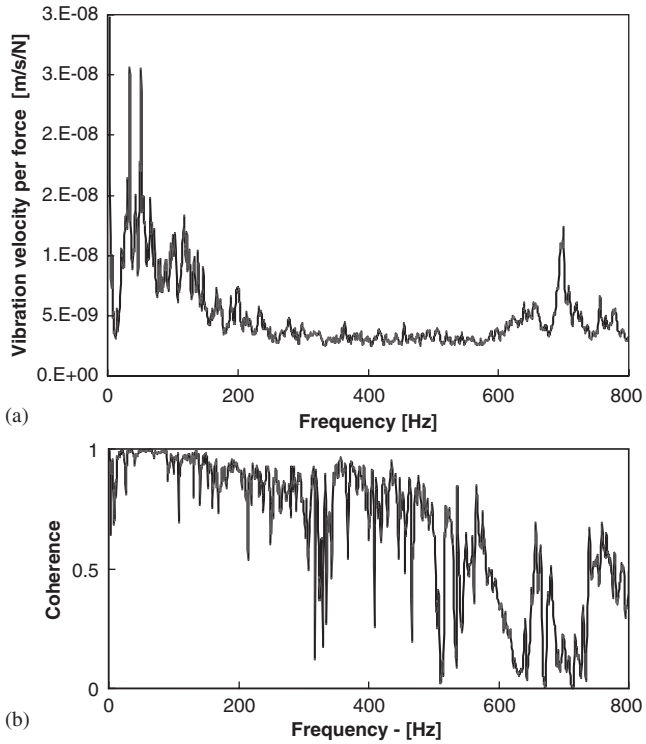

Fig. 3. (a) Average structural frequency response and (b) a typical coherence function of the bridge section.

Eigenfrequencies and mode shapes could also be extracted in the low-frequency range, one of them being depicted in Fig. 4. Considering that vibrations at higher frequencies are much more critical from the point of view of the human ear's sensitivity, it would be more important to identify normal modes at higher frequencies. Unfortunately, due to the relatively low number of measurement points compared with the large dimensions of the structure this was not possible.

2.1.2. Noise radiation measurements

As mentioned in Section 2.1.1, noise radiation measurements have been performed by means of both instrumented and a simple steel hammer. The spectrum of the steel hammer was checked and found to be flat up to 4 kHz, thus by using a reference accelerometer at the excitation point, the frequency range of the measurements could be extended to higher frequencies.

Fig. 5 shows some of the vibro-acoustic transfer functions obtained, characterizing the noise radiation of the bridge. The most important frequency range lies undoubtedly between 630 and 2000 Hz. There is a clear difference between excitations at the intended location of the right and left tracks. Sound radiation upwards and downwards from the deck plate up to 300 Hz is rather similar, irrespective of whether the deck is excited on the right or on the left side, but higher frequency radiation is strongly reduced if excitation and response measurements take place on different sides. One can also observe that the bridge radiates mostly downwards at medium frequencies.

The experimental results can be summarized by saying that the vibro-acoustic response of the bridge, expressed in terms of sound pressure per unit input force, is strongly frequency dependent, with local maxima below 100 Hz, around 630 Hz and from 1250 to 2000 Hz. Being limited in frequency range, the available structural transfer function set is not suited to evaluate whether the important local maxima for medium frequencies are caused by increased vibration in the structure or by increased radiation. In order to investigate the vibro-acoustic behaviour of the bridge in more detail, numerical simulation methods were used and their results compared with the measurements.

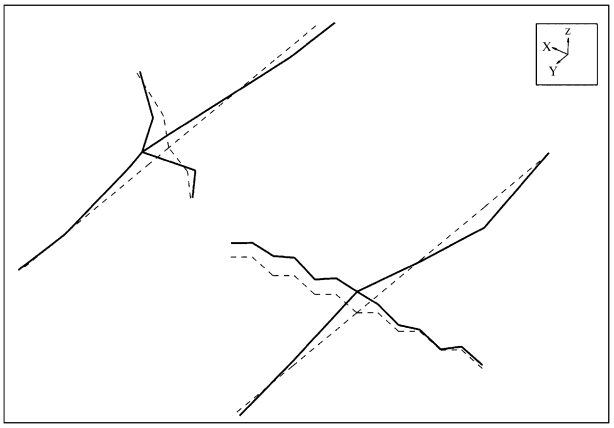

Fig. 4. Experimental mode shape of the 28 Hz normal mode of the investigated bridge section. - - - -, Undeformed structure; ——, deformed mode shape.

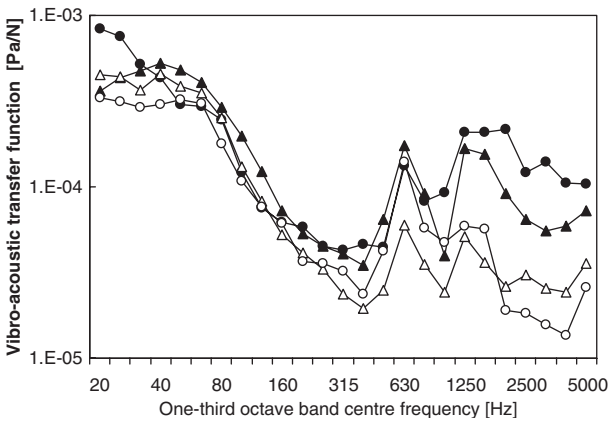

Fig. 5. Vibro-acoustic transfer functions for various excitation and microphone positions. -▲-, Right excitation, microphone 1; -●-, right excitation, microphone 4; -△-, left excitation, microphone 1; -○-, left excitation, microphone 4.

2.2. Numerical simulations

A finite element (FE) model of the investigated section of the bridge was developed and the normal modes were calculated by means of a standard structural FE software package [7]. Fig. 6a shows the FE model and Fig. 6b a typical low-frequency-calculated mode shape, corresponding to the experimental mode shape of Fig. 4. As one would expect, the number of the normal modes obtained is very high, with global modes at very low frequencies and many more local modes just slightly higher. In spite of very long calculation times, the size of the problem was just too big to enable meaningful identification of normal modes above 200 Hz, and hence the causes of the local maxima around 630 Hz and above could not be revealed this way.

Low frequency numerical structural analyses can be extended towards higher frequencies by means of the statistical energy analysis (SEA) method. Various SEA models have been built and analysed by means of a commercial SEA program [8]. In order to enable comparison of various data sets in a common frequency range, these calculations were done for smaller subsystems of the bridge. As an example, the geometry model of the skew side plate of the investigated section is shown in Fig. 7a. Fig. 7b depicts a typical forced response, obtained for a hypothetical 1 N/m line load along the upper edge of the plate, as calculated by means of the FE method.

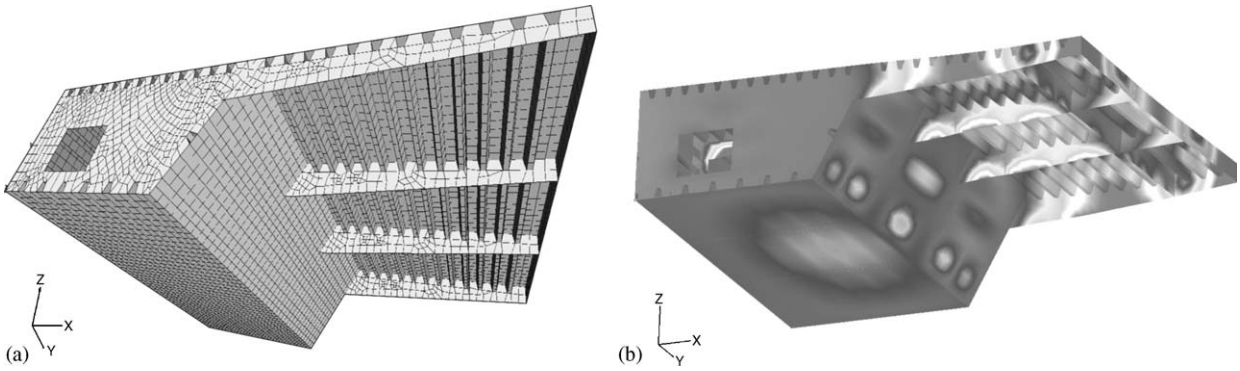

Fig. 6. (a) FE model, and (b) the 28 Hz normal mode of the investigated bridge section, calculated by NASTRAN.

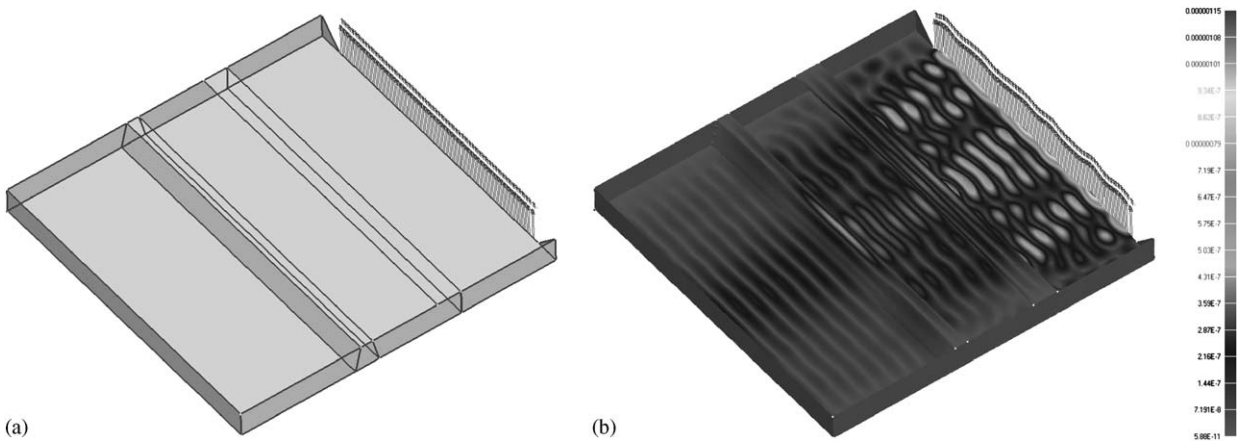

Fig. 7. FE model of the side plate of the investigated bridge section. (a) Geometry of the model, (b) a typical forced response of the plate due to 1 N/m line load along the upper edge of the plate.

Fig. 8 depicts the comparison of measured versus calculated structural responses of this plate. Apart from the oscillatory nature of the FE calculations, the FE and SEA results agree quite well, and the tendency of the experimental results are also similar. (Note that the calculated results refer to 1 N/m load along the upper edge of the skew sideplate of the bridge, while the experimental curve has been derived by applying 1 N point force on the horizontal deck plate, at a distance of app. 5 m from the edge. This explains the considerable shift of the results.) Nevertheless, there is no sign of any increase in the predicted vibration levels at and above 630 Hz whatsoever; the strong noise radiation observed in the experiments does not lend itself to be explained by structural calculations.

The vibro-acoustic phenomena, taking place in and around the bridge structure, have been investigated by calculating the noise radiation efficiencies of the side plate and some other parts of the investigated section by means of a subsequent acoustic boundary element (BE) calculation step. The input of the BE prediction was generated from the FE calculations (forced response displacement are used to generate velocity boundary conditions along a simplified BE mesh). The calculations have been performed by means of SYSNOISE [9], the results are compared in Fig. 9. In order to enable comparison with theoretical data, the radiation efficiency of an infinite steel plate of identical thickness (i.e. 0.01 m) is also drawn.

The radiation efficiency curve calculated for the side plate shows a sharp increase and reaches +10 dB by 1300 Hz. This frequency agrees quite well with the theoretical critical frequency of the plate (1282 Hz) and could explain the local maximum for the 1250 Hz band in Fig. 5. The curve for the cantilever part of the deck plate is less steep and shows local maxima at 250 and 500 Hz. This agreement is less convincing but could help to explain the findings as discussed in Section 2.1.2.

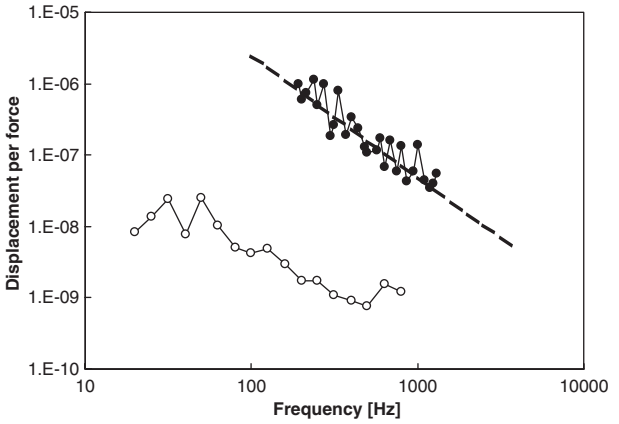

Fig. 8. Comparison of numerical predictions and measurements of structural response along the side plate of the bridge section. Excitation is 1 N/m line load for FE and SEA calculations, and 1 N point force on the deck plate in the experiments; response is expressed in terms of spatial average of displacements along the plate. -●-, FE calculations; — — —, SEA calculations; -○-, experiment.

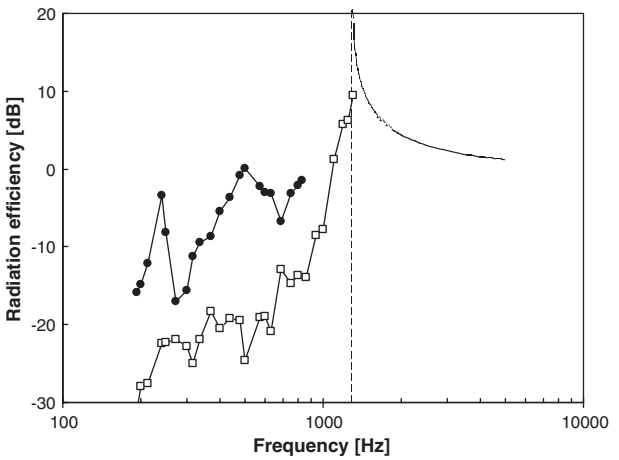

Fig. 9. Calculated radiation efficiencies of various parts of the investigated bridge section. –●–, Deck plate, –□–, skew side plate, full/dashed line: theoretical radiation efficiency of an infinite steel plate of identical thickness.

It is not easy to draw clear-cut conclusions of the vibro-acoustic analysis of the bridge. Nevertheless, it seems to be very likely that the strong low-frequency radiation is generated by structural normal modes of the bridge parts, while the medium-frequency range is governed by vibro-acoustic radiation phenomena of various parts of the system. While good agreement was established for low frequencies and numerical simulations shed light on the vibro-acoustic behaviour of the bridge, none of the structural calculation approaches was found to be entirely apt for predictions at medium frequencies. The prediction was therefore based on a hybrid approach, determining the vibro-acoustic transfer function of the system experimentally.

3. Development of the prediction method

The prediction method developed addresses the structure-borne noise of the track/bridge system only, and consists of three basic steps:

(a) estimation of the expected input force spectrum under real operating conditions as discussed below, the result being the expected force per wheel of the tram;

(b) measurement of the vibro-acoustic transfer function of the bridge between the assumed force input (per box) and near-field points of the sound field (see Section 2.1.2), and
(c) numerical calculation of sound radiation from the near into the far-field, as described in Section 3.2.

Note that neither the airborne component of the rails, nor the noise radiation from the vehicle is tackled in this paper. The rail noise was estimated for the most probable design version of the track and shown to be negligible with respect to the bridge component [2], and the vehicle noise is taken into account by standard traffic noise prediction methods.

3.1. Estimation of the input force of the track

The calculation method is based on a simple single-degree-of-freedom model of the track and wheel (see e.g. in Refs. [4,10]), depicted in Fig. 10. The wheel (including the unsprung mass of the bogie) is represented by the mechanical impedance Z_W of the wheel, while the rail and its underlying structure is substituted by the single rail impedance Z_R. (Note that the contact springs are neglected, and rather than considering the six possible degrees of freedom, just vertical displacements x and velocities v of the elements are included in the model.) The primary source of vibration (and noise) is assumed to be the combined roughness of the contacting surfaces of the wheel and rail, denoted by r in the model. The output of the considered system is the force f_R, exciting the substructure.

On the basis of common electrical analogies it can easily be shown that

$$f_R = \dot{r}(Z_R \times Z_W) = \frac{\dot{r}}{M_R + M_W} = \frac{v_R}{M_R}, \tag{1}$$

where M_R and M_W are the mobility (or mechanical admittance) of the elements in Fig. 10, the dot means time derivative and $\times$ stands for the replus operation.

Suppose that the tram runs along an existing track, where the wheel and rail admittances can readily be measured by means of a simple impact hammer test, and operational rail vibrations are also determined for a number of typical tram passbys [10]. The roughness can then be calculated by simply rearranging Eq. (1). Provided that the same roughness will be present when the tram runs along the bridge, the force f_B exerted on

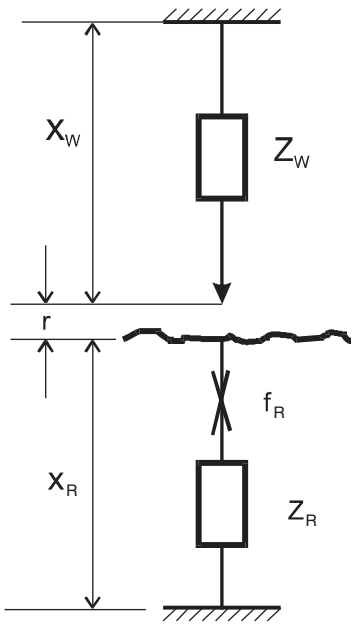

Fig. 10. Single-degree-of-freedom model of the vehicle/contact/rail system.

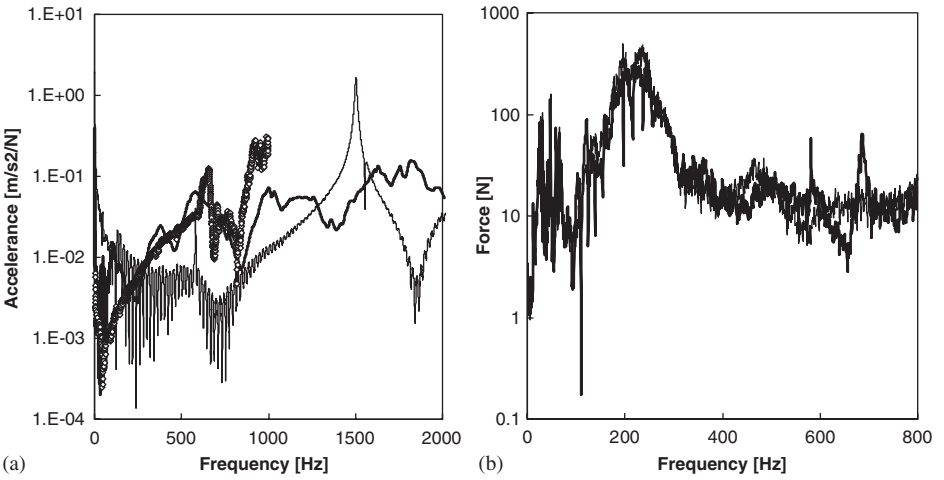

Fig. 11. Estimation of the input force spectrum under real-life operating conditions. (a) Measured accelerances: thick line, on a rail of ballast track; -○-, a point on the deck plate; and —, on the wheels of a TATRA T5C5 tram. (b) Derived force spectrum for a measurement position above rail fixtures on the ballast track (—) and its corrected version according to Eq. (2) (thick line).

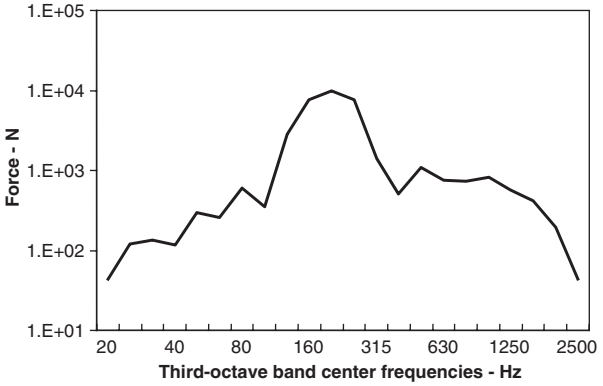

Fig. 12. Force spectrum as in Fig. 11, in one-third octave bands.

the bridge structure can be similarly expressed by

$$f_B = \dot{r}(Z_B \times Z_W) = \frac{v_R}{M_R}\frac{M_R + M_W}{M_B + M_W} = \frac{a_R}{A_R}\frac{A_R + A_W}{A_B + A_W}, \tag{2}$$

where Z_B and A_B is mechanical impedance and mobility of the bridge, a is acceleration and A_R, A_B and A_W are accelerances, measured in terms of acceleration per unit force frequency response functions. Obviously, if the impedance of the bridge is equal to that of any other part of the track, the force will also be identical. Where the substructure is stiffer the force increases, and vice versa.

The measurements were made at three different tracks, where the same type of tram (3-coach train of TATRA T5C5 trams, manufactured for Budapest Transport Ltd.) is in service. The accelerance functions obtained are summarized in Fig. 11a and the force spectra resulting directly from the track measurements and compensated by the differences of the bridge and track mobilities are shown in Fig. 11b and 12 (in one-third octave bands). As can be seen, the force curve has its maximum around 200 Hz which is advantageous, since there is no strong radiation from the bridge in this frequency range.

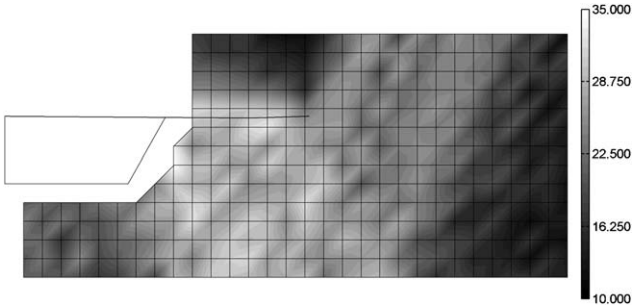

Fig. 13. Predicted sound field between the bridge and façade of the closest building (Palace of Art) for the 1 kHz one-third octave band.

3.2. Sound radiation calculations

The calculation of the noise radiation by means of the BE method is largely limited by the size of the model. Here, meaningful calculations for a full three-dimensional mesh of the bridge section of Fig. 6 were only possible up to 200 Hz, which is by far not sufficient for the problem in question. Therefore, a special statistical two-dimensional version of the BE method was applied [2,11]. A typical field calculation result is shown in Fig. 13 in the form of a sound field map for 1000 Hz, and the average transfer function (or in other words, the sound attenuation) from the near-field microphone positions to the critical point of the Palace of the Arts building are determined as a function of one-third octave bands. It is found that the average value is about 15 dB, with little variation with frequency, hence this value was used for further calculations.

4. Results and evaluation

4.1. Predicted noise without isolation

By using the expected input dynamic force to the deck plate, experimental vibro-acoustic response of the bridge structure and the near-to-far-field sound propagation simulated numerically, the expected level and frequency spectrum of the far-field noise can be synthesized. The worst-case vibro-acoustic transfer function (similar to those functions depicted in Fig. 5) is multiplied by the input force determined for one wheel (as given in Fig. 12), resulting in a hypothetical near-field noise spectrum, see Fig. 14. By assuming that no vibration isolation would be built into the track along the bridge and all wheels of the tram would continuously excite the deck plate by this force irrespective of the number and position of the track-mounting points, the total noise level of the tram passby generated in the near field can be calculated. The next step is to take into account the near/far-field transmission up to the most critical outdoor immission point of the Palace of the Arts, as discussed above. Finally, the total number of tram passbys per calculation period has to be taken into account.

As a result, the A-weighted sound level is estimated to reach 84 dB maximum value for a tram passby along the right track, and $L_{Aeq} = 66.5$ dB for the whole day and 61 dB for the night period is obtained. Based on various considerations as discussed in Section 2 and consulting the investor of the track, it was decided that at least 10 dB noise reduction with respect to the "no isolation" case is required.

4.2. Prediction with isolation

The prediction model developed here is also directly extendable for isolated tracks. Vibration isolated tracks can similarly be approximated as a one-degree-of-freedom mass–spring system, characterized by the resonance frequency of the rail (plus an appropriate amount of the unsprung mass of the wheel set) supported by the used resilient material or element (see Refs. [10,12,13]). Given the required noise reduction and expected noise level without isolation, the selection of the appropriate resonance frequency is a simple optimization task. One potential solution is mentioned and analysed in some detail in Ref. [2].

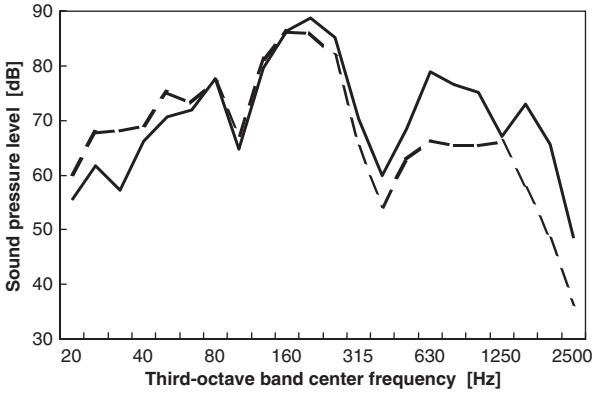

Fig. 14. Predicted noise spectrum, calculated for a full tram passby in the near field of the bridge. Full line: tram on the right (closer), dashed: on the left (farther) track.

5. Summary

A hybrid method, consisting of both in situ measurements and numerical calculations, has been developed to predict the noise radiation of a tram track to be installed onto an existing steel bridge across the Danube in Budapest. The method is composed of three elements: determination of the expected input force, the vibro-acoustic response of the bridge, and the sound propagation from the near field to the immission point.

The vibro-acoustic response of the bridge was investigated by means of structural FE, SEA and acoustic BE calculations, and the calculated results were compared with the results of transfer function measurements. It has been found that both measurements and calculations of a structure of such dimensions are subject to serious limitations, even if just one section of the bridge is considered. Conventional FE and BE methods were able to characterize the whole system up to 100–200 Hz only, while important noise components were to be expected between 500 and 2000 Hz. A vibro-acoustic analysis of some subsystems of the bridge structure has nevertheless revealed important characteristics, such as the presumable reason of the strong radiation in the 630 and 1250 Hz band. It seems that the behaviour of the bridge is determined by global normal modes of the system at low frequencies, and by vibro-acoustic effects for medium frequencies, these latter ones being dominant for the overall *A*-weighted level.

The prediction was performed first by assuming a rigid connection between the rail and the bridge. The expected dynamic input force of the track were derived from measurements at other locations and the vibro-acoustic transfer functions were determined between the deck plate and near-field microphone positions experimentally. The sound propagation characteristics from near to far-field were derived by means of a special two-dimensional BE technique. It was established that the structure-borne component of the tram noise should be reduced by at least 10 dB.

Although not reported here in detail, it was also mentioned that the prediction model can readily be extended to predict isolated track systems. A trial calculation has shown that the targeted noise reduction can be achieved by appropriately resilient support elements in the track.

References

[1] S. Domanovszky, The construction of the Danube-bridge's steel deck, *Közlekedésépítés- és Mélyépítéstudományi Szemle (Scientific Revue of Civil Engineering)* XLV (10–11) (1995) 409–428 (in Hungarian).

[2] F. Augusztinovicz, F. Márki, K. Gulyás, A.B. Nagy, P. Fiala, Vibro-acoustic design of a tram track for a steel road bridge, in: *CD Proceedings of Internoise 2004*, Paper No. 791, Prague, Czech Republic, 2004.

[3] F. Augusztinovicz, F. Márki, P. Carels, M. Bite, I. Dombi, Noise and vibration control of the South railway bridge of Budapest, in: *CD-ROM Proceedings of the 11th International Congress on Noise and Vibration*, Stockholm, Sweden, 2003.

[4] D.J. Thompson, Wheel–rail noise generation, Part I to V, *Journal of Sound and Vibration* 161 (3) (1993) 387–482.

[5] M.H.A. Janssens, D.J. Thompson, A calculation model for the noise from steel railway bridges, *Journal of Sound and Vibration* 193 (1) (1996) 295–304.
[6] J.G. Walker, N.S. Ferguson, M.G. Smith, An investigation of noise from trains on bridges, *Journal of Sound and Vibration* 193 (1) (1996) 307–314.
[7] MSC.VisualNastran for Windows 2002, MSC.Software Corp., 2002.
[8] Statistical Energy Analysis program package SEADS, Rev. 1.2 LMS International, Leuven, 2002.
[9] Vibro-acoustic prediction software package SYSNOISE, Rev. 5.6 LMS International, Leuven, 2004.
[10] A.P. de Man, A Survey of Dynamic Railway Track Properties and their Quality, PhD Thesis, Technische Universiteit Delft, 2002.
[11] F. Márki, F. Augusztinovicz, Statistical—inverse boundary element method, in: *CD Proceedings of the 27th International Seminar on Modal Analysis*, Leuven, 2002.
[12] R.G. Wettschurek, R.J. Diehl, The dynamic stiffness as an indicator of the effectiveness of a resilient rail fastening system applied as a noise mitigation measure: laboratory tests and field application, *Rail Engineering International* 4 (2000) 7–10.
[13] CDM Vibration Isolation Systems, *CD ROM Version 1.4*, CDM nv, Belgium, 2001.